Copyright © 2006 Tech Science Press CMES, vol.16, no.3, pp.197-208, 2006

Wave Propogation Characteristics of Rotating Uniform Euler-Bernoulli Beams

K.G. Vinod[1], S. Gopalakrishnan[1] and R. Ganguli[1]

Abstract: A spectral finite element formulation for a rotating beam subjected to small duration impact is presented in this paper. The spatial variation in centrifugal force is modeled in an average sense. Spectrum and dispersion plots are obtained as a function of rotating speed. It is shown that the flexural wave tends to behave non-dispersively at very high rotation speeds. The numerical results are simulated for two rotating waveguides of different dimensions. The results show that there is a steep increase in responses with the response peaks and the reflected signals almost vanishing at higher rotating speeds. The solution obtained in this work can be used as Ritz functions for the spectral finite element method, where the variable coefficient differential equation is present.

keyword: Wavenumber, spectrum relation, non-dispersive, group speed, phase speed, transfer function, Lagrangian.

1 Introduction

The problem of determining vibration characteristics of rotating beams is a requirement in various branches of engineering. The determination of the structural response and modal frequencies are essential in the design of rotating structural elements such as helicopter blades, airplane propellers and turbo machinery blades. Such beams can also be present as elements of complexmulti-body dynamic systems (Huston and Liu (2005)). The analysis of these structural elements leads to differential equations with variable coefficients; which are introduced due to the variation of centrifugal force and geometry along the beam length. In general, rotation complicates the analysis of engineering structures (Leu and Chen (2006)). A number of solution techniques, with varying degrees of applicability have been suggested in the literature for the rotating beam problem. Wright, Smith, Thresher, and Wang (1982) used the Frobenius method to get the exact frequencies and mode shapes of a rotating beam with linear variation in flexural rigidity and mass along the length. Naguleswaran (1994), presented the dimensionless natural frequencies of a rotating beam for different boundary conditions. He solved the mode shape equation by the Frobenius method and the frequency equations by trial and error. Banerjee (2000) derived the dynamic stiffness matrix of a non-uniform, rotating, Euler-Bernoulli beam using the Frobenius method of solution in power series. He also modeled a tapered beam assembling the dynamic stiffness matrices of uniform beams by approximating the tapered beam as an assembly of many different uniform beams.

The finite element method has emerged as the analysis technique of choice in recent years (Forth and Staroselsky (2005), Andreaus, Batra, and Porfiri (2005), Fedelinski and Gorski (2006)). Several finite element method based approaches for rotating beams have also been discussed in the literature. Nagaraj and Kumar (1975) used Galerkin FEM for finding the vibration characteristics of the rotating beam. Hoa (1979) analyzed the vibration frequencies of a rotating beam with a tip mass using the finite element method, where he assumed a third order polynomial for the lateral displacement. Putter and Manor (1978) found the lead lag natural frequencies of a radial beam mounted on a rotating disc using FE technique and he used a fifth degree polynomial as the displacement function. The convergence of the FE model depends on the number of elements used. That is, even for obtaining the lower mode frequencies, a large size eigenvalue problem needs to be solved. Furthermore, a very large number of finite elements are required for determining the higher mode frequencies.

Impact loads of small duration are normally encountered in many rotating systems such as helicopter blades. Some typical examples are the bird hit on helicopter or turbine/compressor blades. Alternatively, such short duration pulses are required, if one has to perform structural health monitoring studies. Short duration pulses excite many higher order modes. In order to capture these higher order modes accurately, it is necessary that

[1] Department of Aerospace Engineering, Indian Institute of Science, Bangalore-560012, India

element sizes shall be very small, of the order of the wavelength of signal. This will increase the computation cost of conventional finite element method (CFEM) enormously. Spectral finite element method (SFEM) is an efficient technique for this case to achieve high accuracy using a limited number of elements, because in most cases, it uses exact solution to the governing differential equation in the frequency domain, as the interpolating functions for element formulation (Wu, Liu, Scarpas, and Ge (2006), Mitra and Gopalakrishnan (2006)). As a result, the spectral element treats the distribution of mass and rotational inertia of the structural element exactly. Only one spectral element needs be placed between any two joints, substantially reducing the total number of degrees of freedom in the system. The spectral formulation requires that the assembled system of equations be solved in the frequency domain and utilizes the Fast Fourier Transform (FFT) to transform the time domain responses to the frequency domain and back. Spectral element method was originally proposed by Narayanan and Beskos (1982) and popularized by Doyle (1989). Spectral element for elementary isotropic waveguides was formulated by Doyle (1988), Doyle and Farris (1990) and higher order waveguides by Gopalakrishnan, Martin, and Doyle (1992) and Martin, Gopalakrishanan, and Doyle (1994). Similarly, spectral element for elementary and higher order composite waveguides were formulated by Mahapatra and Gopalakrishnan (2000) and Mahapatra and Gopalakrishnan (2003). Spectral elements for inhomogenous waveguides were formulated by Chakraborty and Gopalakrishnan (2003), Chakraborty and Gopalakrishnan (2005). These works show the versatility of spectral FEM in handling high frequency impact type load. Similar wave based methods are finding increasing applications in the recent literature (Han, Ding, and Liu (2005), Pluymers, Desmet, Vandepitte, and Sas (2005))

In the present work, the response of a beam with centrifugal force, subjected to a transverse impact load is studied using the spectral FEM. The governing partial differential equation for a uniform rotating beam is derived using Hamilton's principle and the variable coefficient for the centrifugal term is replaced by the maximum centrifugal force. The rotating beam problem is now transformed to a case of beam subjected to an axial force. Even though this averaging seems to be a crude approximation, one can use this as a powerful model in analyzing the wave propagation characteristics of the rotating structure. Furthermore, the solutions can be used as Ritz functions for spectral finite element analysis of the variable coefficient differential equation. The constant coefficient PDE is solved using spectral analysis. The beam is subjected to an impact load and the effect of axial force due to rotation and flexural stiffness on the structure response, spectrum relation and response amplitude is studied qualitatively and presented.

2 Mathematical formulation

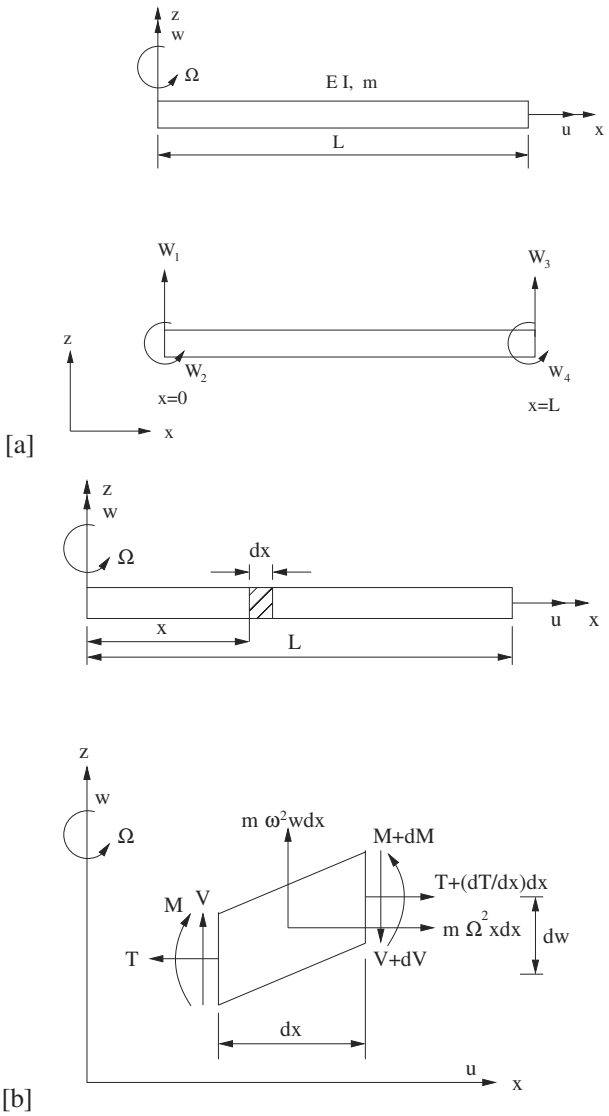

Figure 1 : (a)Spectral finite element for a beam under rotation, (b) Forces acting on an incremental length *dx* of the rotating beam

A rotating blade can be represented as a cantilever beam having vibration displacements perpendicular to the plane of rotation (flapping motion). Considering the elementary theory of beams, the axial and transverse displacement fields of a rotating blade can be represented as a cantilever beam having vibration displacements perpendicular to the plane of rotation (flapping motion). Considering the elementary theory of beams, the axial and transverse displacement fields are

$$u(x,y,z,t) = u_0(x,t) - z\frac{\partial w(x,t)}{\partial x} \tag{1}$$

$$w(x,y,z,t) = w(x,t) \tag{2}$$

The strain

$$\varepsilon_{xx} = \frac{\partial u_0}{\partial x} - z\frac{\partial^2 w}{\partial x^2} \tag{3}$$

The governing equation can be derived from the Hamilton's principle where the action integral $\int_{t_1}^{t_2} L dt$ assumes a stationary value. ie. $\delta\int_{t_1}^{t_2} L dt = 0$, where L is the Lagrangian given as

$$L = (T - V) \tag{4}$$

The total kinetic energy of the beam is

$$\begin{aligned} T &= \frac{1}{2}\int_0^L \left[\rho A(x)\left(\left(\frac{\partial u_0}{\partial t} - z\frac{\partial}{\partial t}\left(\frac{\partial w}{\partial x}\right)\right)^2 + \left(\frac{\partial w}{\partial t}\right)^2\right) \right. \\ &\quad \left. + \frac{1}{2}m(\Omega x)^2\right] dx \\ &= \frac{1}{2}\int_0^L \left[\rho A(x)\left(\left(\frac{\partial u_0}{\partial t}\right)^2 + \left(\frac{\partial w}{\partial t}\right)^2\right) + \frac{1}{2}m(\Omega x)^2\right] dx \end{aligned} \tag{5}$$

where ρ is the mass density, A is the beam cross section area, I is the moment of inertia and Ω is the rotation speed.

The total potential energy is

$$\begin{aligned} V &= \frac{1}{2}E\int_V \varepsilon_{xx}^2 dV + \int_0^L \frac{1}{2}T(x)\left(\frac{\partial w}{\partial x}\right)^2 dx \\ &= \int_0^L \frac{EA(x)}{2}\left(\frac{\partial u_0}{\partial x}\right)^2 dx + \int_0^L \frac{EI(x)}{2}\left(\frac{\partial^2 w}{\partial x^2}\right)^2 dx \\ &\quad + \int_0^L \frac{1}{2}T(x)\left(\frac{\partial w}{\partial x}\right)^2 dx \end{aligned} \tag{6}$$

On substituting Eq. 5 and Eq. 6 in Eq. 4 and using the Hamilton's principle, we get the governing differential equation for transverse displacement $w(x,t)$ as

$$\frac{\partial^2}{\partial x^2}\left(EI(x)\frac{\partial^2 w}{\partial x^2}\right) - \frac{\partial}{\partial x}\left(T(x)\frac{\partial w}{\partial x}\right) + \rho A(x)\frac{\partial^2 w}{\partial t^2} = 0 \tag{7}$$

where $T(x)$ is the axial force due to centrifugal stiffening and is given as

$$T(x) = \int_x^L \rho A(x)\Omega^2 x dx \tag{8}$$

For a uniform, isotropic beam, Eq. 7 reduces to

$$EI\frac{\partial^4 w}{\partial x^4} - \frac{\partial}{\partial x}\left(T(x)\frac{\partial w}{\partial x}\right) + \rho A\frac{\partial^2 w}{\partial t^2} = 0 \tag{9}$$

For the spectral FEM formulation, we assume a uniform beam and replace $T(x)$ by the maximum force (at the root, i.e. at $x = 0$)

$$T_{max} = \int_0^L \rho A(x)\Omega^2 x dx = \frac{\rho A\Omega^2 L^2}{2} \tag{10}$$

This allows us to represent Eq. 9 as a constant coefficient PDE which can be written as

$$EI\frac{\partial^4 w}{\partial x^4} - T_{max}\frac{\partial^2 w}{\partial x^2} + \rho A\frac{\partial^2 w}{\partial t^2} = 0 \tag{11}$$

The above PDE (Eq. 11) governs the transverse displacement of a beam with axial load undergoing out of plane motion. In this particular problem, the axial load is proportional to the rotation speed. Though approximate, this mathematical model can give significant insight into the study of spectrum relations of a rotating beam. The main objective of the paper is to obtain Ritz functions for solving the variable coefficient partial differential equation representing the exact variation of centrifugal force and to see how the axial force affects the overall wave propagation behavior of rotating beams.

3 Spectral finite element formulation

Spectral formulation begins by representing the transverse displacement $w(x,t)$ of the beam in spectral form as

$$w(x,t) = \sum_{n=1}^{N} \hat{w}_n(x,\omega_n)e^{i\omega_n t} \tag{12}$$

where ω_n the circular frequency of the n^{th} sampling point and N is the Nyquist frequency. The sampling rate and the number of sampling points (N_1) should be sufficiently large to have relatively good resolution of both high and low frequencies respectively. On substituting Eq. 12 in Eq. 11 we get,

$$\sum_{n=1}^{N}\left[EI\frac{\partial^4\hat{w}_n}{\partial x^4}-T_{max}\frac{\partial^2\hat{w}_n}{\partial x^2}+\rho A(i\omega_n)^2\hat{w}_n\right]e^{i\omega_n t}=0 \quad (13)$$

The Eq. 13 must be satisfied for each n and hence can be written as

$$EI\frac{\partial^4\hat{w}_n}{\partial x^4}-T_{max}\frac{\partial^2\hat{w}_n}{\partial x^2}-\rho A\omega_n^2\hat{w}_n=0 \quad (14)$$

Since the differential equation is a constant coefficient one, it has the solution of the form $\hat{w}_n=e^{-ik_nx}$. On substituting this solution in Eq.(14) we get,

$$k_n^4+\frac{T_{max}}{EI}k_n^2-\frac{\rho A\omega_n^2}{EI}=0 \quad (15)$$

where k_n is the wavenumber, which can be obtained as

$$k_{pn}=\pm\sqrt{\frac{-\left(\frac{\rho A\Omega^2L^2}{2EI}\right)\pm\sqrt{\left(\frac{\rho A\Omega^2L^2}{2EI}\right)^2+\left(\frac{4\rho A\omega_n^2}{EI}\right)}}{2}} \quad (16)$$

Since Eq. 14 is a fourth order equation, we get four solutions of which two are purely real and the other two are purely imaginary. The subscript p corresponds to the different modes of wave propagation. The real part gives rise to the propagating component while the imaginary part gives rise to the spatially damped mode. From Eq. 16 it is obvious that, there is no possibility for a cut off frequency, above which the spatially damped mode turns to be propagative. The above relation (Eq. 16) between the wavenumber k_n and frequency ω_n is called the spectrum relation and for a beam, it is a nonlinear function of frequency. Thus the phase speed which is defined as $c=\frac{\omega_n}{(k_n)_R}$ is different for different ω_n. In addition, it should be noted that the phase speed is defined with respect to real k_n, since the real part represents the propagative component of the wave. As a result, the speeds change with frequencies, which makes the wave highly dispersive. The group speeds can be evaluated using the expression $c_g=\frac{d\omega}{dk}$. This is the speed one has to use for calculating the arrival of reflections.

Due to the inherent periodicity in wave analysis, it is common that the signals from the neighboring window propagates into view from the left, if the time window ($N_1\Delta t$) selected is not adequate. This will become prominent for a dispersive system; say for beams, where the low frequency components take an infinitely long time to propagate into view. Thus the response will remain until the time reaches infinity. This windowing problem exists even for very high values of N_1 and can be solved in a computationally cheaper way by adding damping to the system, so that all the signals eventually die out within the chosen window. Mathematically, damping makes the wavenumber complex and each term in the wave solution is multiplied by a $e^{-\frac{\eta}{EI}x}$term. The governing PDE with added damping in the spectral form is

$$EI\frac{\partial^4\hat{w}_n}{\partial x^4}-T_{max}\frac{\partial^2\hat{w}_n}{\partial x^2}-\rho A\omega_n^2\hat{w}_n+i\omega_n\eta\hat{w}_n=0 \quad (17)$$

4 Non-Dimensional form

To express the PDE in a non-dimensional form, we define

$$X=\frac{x}{L};\ \overline{W}=\frac{w}{L};\ \frac{d\hat{w}}{dx}=\frac{d\overline{W}}{dX};\ L\frac{d^2\hat{w}}{dx^2}=\frac{d^2\overline{W}}{dX^2};$$
$$L^2\frac{d^3\hat{w}}{dx^3}=\frac{d^3\overline{W}}{dX^3};\ L^3\frac{d^4\hat{w}}{dx^4}=\frac{d^4\overline{W}}{dX^4} \quad (18)$$

$$\left\{\frac{d^4\overline{W}}{dX^4}-\left(\frac{\Omega^2}{\frac{2EI}{\rho AL^4}}\right)\frac{d^2\overline{W}}{dX^2}-\left(\frac{\omega_n^2}{\frac{EI}{\rho AL^4}}\right)\overline{W}+i\left(\frac{\omega_n}{\frac{EI}{\eta L^4}}\right)\overline{W}\right\}=0 \quad (19)$$

Defining

$$\frac{EI}{\rho AL^4}=\omega_{str}^2;\ \frac{\eta\omega_n}{\rho A}=\psi^2 \quad (20)$$

$$\left\{\frac{d^4\overline{W}}{dX^4}-\frac{1}{2}\left(\frac{\Omega}{\omega_{str}}\right)^2\frac{d^2\overline{W}}{dX^2}-\left(\frac{\omega_n}{\omega_{str}}\right)^2\overline{W}+i\left(\frac{\psi}{\omega_{str}}\right)^2\overline{W}\right\}=0 \quad (21)$$

Let $\overline{W}=e^{-i\overline{k}_nX}$ be the solution, then

$$\overline{k}_{pn}=\pm0.707\left[-\frac{1}{2}\left(\frac{\Omega}{\omega_{str}}\right)^2\pm\left\{\frac{1}{4}\frac{\Omega^4}{\omega_{str}^4}-4\left(-\frac{\omega_n^2}{\omega_{str}^2}+i\frac{\psi^2}{\omega_{str}^2}\right)\right\}^{1/2}\right]^{1/2} \quad (22)$$

The solution of Eq. 21 can be written as

$$\overline{W}(X) = \left\{ C_1 e^{-i\overline{k}_1 X} + C_2 e^{-i\overline{k}_4 X} + C_3 e^{i\overline{k}_2(1-X)} + C_4 e^{i\overline{k}_3(1-X)} \right\} \tag{23}$$

where $\overline{k}_1$ and $\overline{k}_2$ are the positive and negative real roots and $\overline{k}_3$ and $\overline{k}_4$ are the positive and negative imaginary roots.Then

$$\overline{W}(X,\overline{t}) = \sum_{n=1}^{N} \left[C_{1n} e^{-i\overline{k}_{1n} X} + C_{2n} e^{-i\overline{k}_{4n} X} + C_{3n} e^{i\overline{k}_{2n}(1-X)} + C_{4n} e^{i\overline{k}_{3n}(1-X)} \right] e^{i\overline{\omega}_n \overline{t}} \tag{24}$$

Defining the displacement boundary conditions in the frequency domain as

$$at\, X = 0,\ \overline{W}(0) = \overline{W}_1,\ \ \overline{W}'(0) = \overline{W}_2 \tag{25}$$

$$at\, X = 1,\ \overline{W}(1) = \overline{W}_3,\ \ \overline{W}'(1) = \overline{W}_4 \tag{26}$$

$$\overline{W}_1 = C_1 + C_2 + C_3 e^{i\overline{k}_2} + C_4 e^{i\overline{k}_3} \tag{27}$$

$$\overline{W}_2 = -i\overline{k}_1 C_1 - i\overline{k}_4 C_2 - i\overline{k}_2 C_3 e^{i\overline{k}_2} - i\overline{k}_3 C_4 e^{i\overline{k}_3} \tag{28}$$

$$\overline{W}_3 = C_1 e^{-i\overline{k}_1} + C_2 e^{-i\overline{k}_4} + C_3 + C_4 \tag{29}$$

$$\overline{W}_4 = -i\overline{k}_1 C_1 e^{-i\overline{k}_1} - i\overline{k}_4 C_2 e^{-i\overline{k}_4} - i\overline{k}_2 C_3 - i\overline{k}_3 C_4 \tag{30}$$

$$\{\overline{W}\} = \begin{pmatrix} \overline{W}_1 \\ \overline{W}_2 \\ \overline{W}_3 \\ \overline{W}_4 \end{pmatrix} = [\overline{A}] \begin{pmatrix} C_1 \\ C_2 \\ C_3 \\ C_4 \end{pmatrix} \tag{31}$$

where,

$$[\overline{A}] = \begin{pmatrix} 1 & 1 & e^{i\overline{k}_2} & e^{i\overline{k}_3} \\ -i\overline{k}_1 & -i\overline{k}_4 & -i\overline{k}_2 e^{i\overline{k}_2} & -i\overline{k}_3 e^{i\overline{k}_3} \\ e^{-i\overline{k}_1} & e^{-i\overline{k}_4} & 1 & 1 \\ -i\overline{k}_1 e^{-i\overline{k}_1} & -i\overline{k}_4 e^{-i\overline{k}_4} & -i\overline{k}_2 & -i\overline{k}_3 \end{pmatrix}$$

$$\{\overline{W}\} = [\overline{A}]\,\{\overline{C}\} \tag{32}$$

Defining the non-dimensional forces and moments as

$$\frac{d^3\overline{W}}{dX^3} = \hat{F}\left(\frac{L^2}{EI}\right) = \frac{\hat{F}}{\omega_{str}^2 mL}$$
$$\frac{d^2\overline{W}}{dX^2} = \hat{M}\left(\frac{L}{EI}\right) = \frac{\hat{M}}{\omega_{str}^2 mL^2} \tag{33}$$

Defining the force boundary conditions

$$at\, X = 0,\ \frac{d^3\overline{W}}{dX^3} = \frac{\hat{F}_1}{\omega_{str}^2 mL};\ \frac{d^2\overline{W}}{dX^2} = \frac{\hat{M}_1}{\omega_{str}^2 mL^2} \tag{34}$$

$$at\, X = 1,\ \frac{d^3\overline{W}}{dX^3} = \frac{\hat{F}_2}{\omega_{str}^2 mL};\ \frac{d^2\overline{W}}{dX^2} = \frac{\hat{M}_2}{\omega_{str}^2 mL^2} \tag{35}$$

$$\frac{\hat{F}_1}{\omega_{str}^2 mL} = i\overline{k}_1^3 C_1 + i\overline{k}_4^3 C_2 + i\overline{k}_2^3 C_3 e^{i\overline{k}_2} + i\overline{k}_3^3 C_4 e^{i\overline{k}_3} \tag{36}$$

$$\frac{\hat{M}_1}{\omega_{str}^2 mL^2} = -(-\overline{k}_1^2 C_1 - \overline{k}_4^2 C_2 - \overline{k}_2^2 C_3 e^{i\overline{k}_2} - \overline{k}_3^2 C_4 e^{i\overline{k}_3}) \tag{37}$$

$$\frac{\hat{F}_2}{\omega_{str}^2 mL} = -i\overline{k}_1^3 C_1 e^{-i\overline{k}_1} - i\overline{k}_4^3 C_2 e^{-i\overline{k}_4} - i\overline{k}_2^3 C_3 - i\overline{k}_3^3 C_4 \tag{38}$$

$$\frac{\hat{M}_2}{\omega_{str}^2 mL^2} = -\overline{k}_1^2 C_1^{-i\overline{k}_1} - \overline{k}_4^2 C_2 e^{-i\overline{k}_4} - \overline{k}_2^2 C_3 - \overline{k}_3^2 C_4 \tag{39}$$

$$\{\overline{F}\} = \begin{pmatrix} \hat{F}_1 L \\ \hat{M}_1 \\ \hat{F}_2 L \\ \hat{M}_2 \end{pmatrix} \left(\frac{1}{\omega_{str}^2 mL^2}\right) = [\overline{B}] \begin{pmatrix} C_1 \\ C_2 \\ C_3 \\ C_4 \end{pmatrix} \tag{40}$$

where,

$$[\overline{B}] = \begin{pmatrix} i\overline{k}_1^3 & i\overline{k}_4^3 & i\overline{k}_2^3 e^{i\overline{k}_2} & i\overline{k}_3^3 e^{i\overline{k}_3} \\ \overline{k}_1^2 & \overline{k}_4^2 & \overline{k}_2^2 e^{i\overline{k}_2} & \overline{k}_3^2 e^{i\overline{k}_3} \\ -i\overline{k}_1^3 e^{-i\overline{k}_1} & -i\overline{k}_4^3 e^{-i\overline{k}_4} & -i\overline{k}_2^3 & -i\overline{k}_3^3 \\ -\overline{k}_1^2 e^{-i\overline{k}_1} & -\overline{k}_4^2 e^{-i\overline{k}_4} & -\overline{k}_2^2 & -\overline{k}_3^2 \end{pmatrix}$$

$$\{\overline{F}\} = [\overline{B}]\,\{\overline{C}\} \tag{41}$$

But from Eq.(32)

$$\{C\} = [A]^{-1}\,\{\overline{W}\} \tag{42}$$

Substituting Eq.(42) in Eq.(41)

$$\{\overline{F}\} = \left[\overline{B}\right]\left[\overline{A}\right]^{-1}\{\overline{W}\}$$

$$\left[\overline{K}\right] = \left[\overline{B}\right]\left[\overline{A}\right]^{-1} \tag{43}$$

Thus $\left[\overline{K}\right]$ is the non-dimensional dynamic stiffness matrix in frequency domain.

$$\overline{F}\} = \left[\overline{K}\right]\{\overline{W}\} \tag{44}$$

The response at the nodes in the frequency domain is $\{\overline{W}\} = \left[\overline{K}\right]^{-1}\{\overline{F}\}$. Here $\left[\overline{K}\right]^{-1}$ is the system transfer function, represented as G. Applying the cantilever boundary conditions, the reduced form of equation is given as

$$\begin{pmatrix} \overline{W}_3 \\ \overline{W}_4 \end{pmatrix} = \begin{pmatrix} \overline{G}_{33} & \overline{G}_{34} \\ \overline{G}_{43} & \overline{G}_{44} \end{pmatrix} \begin{pmatrix} \overline{F}_2 \\ \overline{M}_2 \end{pmatrix} \tag{45}$$

To find the response at $X = 1$, when subjected to an impact load at the same location, the above matrix further reduces to

$$\overline{W}_3 = \overline{G}_{33}\overline{F}_2 \tag{46}$$

The response at any location X can be found by

$$\overline{W}(X) = [\ e^{-i\overline{k}_1 X} \quad e^{-i\overline{k}_4 X} \quad e^{i\overline{k}_2(1-X)} \quad e^{i\overline{k}_3(1-X)}\ ]\{\overline{C}\} \tag{47}$$

Defining

$$\overline{\omega}_n = \frac{\omega_n}{\omega_1};\ \overline{t} = t\omega_1;\ \overline{v} = \frac{v}{L\omega_1} \tag{48}$$

where ω_1 is the first sampling frequency or the lowest harmonic considered in the response spectrum. The non-dimensional phase speed and group speed is defined as

$$\overline{c}_n = \frac{\overline{\omega}_n}{(\overline{k}_n)_R}$$

$$\overline{c}_g = \frac{d\overline{\omega}_n}{d(\overline{k}_n)_R} \tag{49}$$

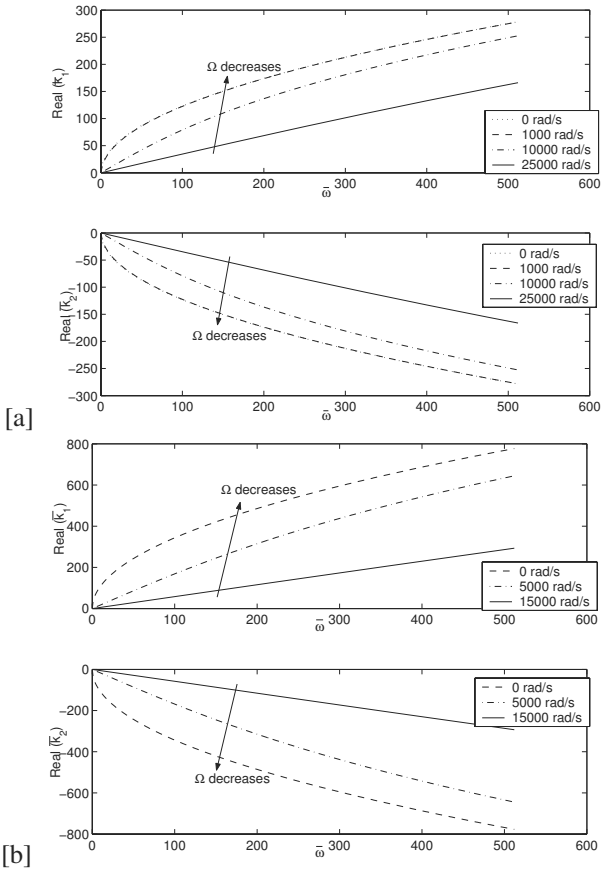

Figure 2 : Variation of $\overline{k}$ wrt. $\overline{\omega}$ for different Ω , keeping ω_{str} constant(a) Euler beam1, L 0.6m, mass 1.128kg, ω_{str} 40.5 rad/s,ω_1 (first sampling frequency) 6.136$e3rad/s$ (b) Euler beam2, L 4.94m, mass 31.924kg,ω_{str} 5.198rad/s ,ω_1 6.136$e3rad/s$

5 Numerical Results

Two uniform isotropic beams of length 0.6m and 4.94m are taken as examples. Properties of the two beams are given in Tab. 1 (Pawar and Ganguli (2003)). The aim is to bring out the difference in wave propagation behavior of these structural elements qualitatively, at different rotation speeds/axial forces. So, the material failure due to high stress is not considered in this study. All the cases presented here are for a given mass and length.

5.1 Spectrum relations

5.1.1 Case1(Keeping ω_{str} fixed and vary Ω)

The non-dimensional real wavenumbers $\overline{k}_1$ and $\overline{k}_2$ are plotted against non-dimensional frequency $\overline{\omega}$, for differ-

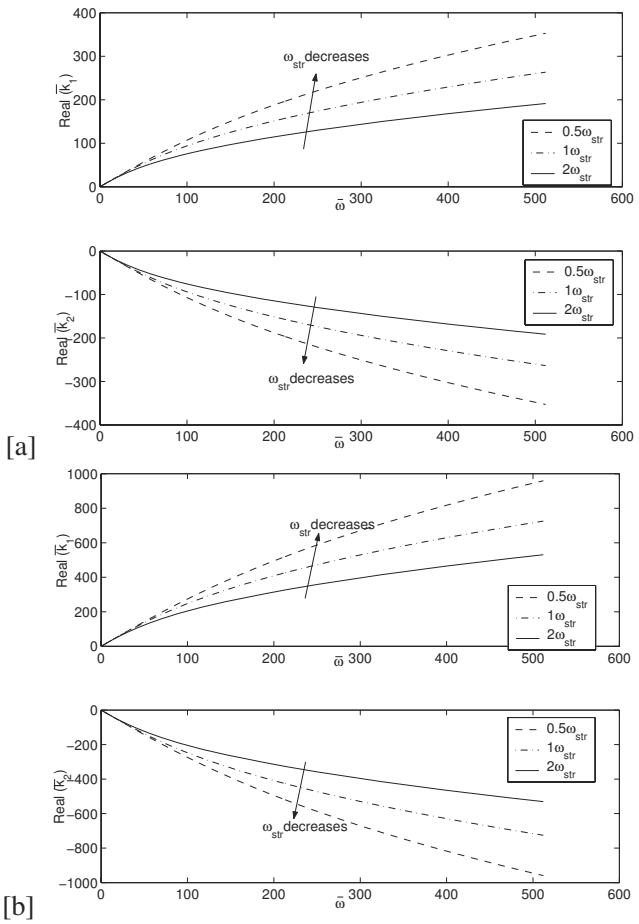

Figure 3 : Variation of $\overline{k}$ wrt. $\overline{\omega}$ for different ω_{str}, (0.5 1 2)ω_{str} keeping Ω constant (a)Euler beam1, L $0.6m$, mass $1.128kg$, Ω $7500rad/s$, ω_{str} $40.5rad/s$, ω_1 (first sampling frequency) $6.136e3rad/s$ (b) Euler beam2, L $4.94m$, mass $31.924kg$, Ω $3000rad/s$, ω_{str} $5.198rad/s$, ω_1 $6.136e3rad/s$

Table 1 : Beam properties

Euler Bernoulli beam1	
Length, m	0.6
Cross sectional area, m^2	240 x 10^{-6}
Moment of Inertia, m^4	2000 x 10^{-12}
E, GPa	200
Mass density, kg/m^3	7840
Euler Bernoulli beam2	
Length, m	4.94
Mass per unit length, ρA, kg/m	6.46
$\frac{EI_y}{\rho A\omega^2 L^4}$	0.0168

ent Ω, keeping ω_{str} fixed. Fig. 2 indicates a quadratic relationship between $\overline{k}$ and $\overline{\omega}$ at zero or lower rotation speeds. In Fig. 2a the wavenumber plots corresponding to $\Omega = 0$ and $1000rad/s$ are lying together. At high rotation speeds, the spectrum relation becomes linear or otherwise, the waves become non-dispersive. Also, the wavenumber shows an inverse dependence on rotation speed. For a non-rotating Euler-Bernoulli beam, the spectrum relation $\overline{k}_n = \sqrt{\omega_n}(\frac{\rho A}{EI})^{\frac{1}{4}}$ is dispersive in nature. But for a rotating beam, at higher speeds, the above nonlinear relation shifts to a linear nature due to the relatively negligible contribution from the ω_n term, especially for lower values of ω_n . That is, the variation of $\overline{k}_n$ is dominated by the centrifugal force term at high Ω.

5.1.2 Case 2 (Keeping Ω fixed and vary ω_{str})

The non-dimensional real wavenumbers $\overline{k}_1$ and $\overline{k}_2$ are plotted against non-dimensional frequency $\overline{\omega}$, for different ω_{str}, keeping Ω constant. From Fig. 3 it is apparent that as ω_{str} goes up; i.e. as EI increases for a given mass and length of the beam, the wavenumber decreases and becomes more quadratic. The reason is quite obvious from Eq. 22, since ω_{str} is in the denominator.

5.2 Dispersion relations

5.2.1 Case 1 (Keeping ω_{str} fixed and vary Ω)

Generally, for beams, different frequency components travel at different speeds. Fig. 4 shows that, for a non-rotating beam, the group speed is double the phase speed. Also, c and c_g rises with rotating speed and the difference between them dips at high Ω. This is due to the reduction in the wavenumber at high Ω, as observed in the previous section. As the limiting case, we can say that they become equal and become constant for all ω_n. For a non-rotating beam, both c and c_g are dispersive and shows that the speeds approach infinity for very high frequencies. This unreasonable limit is due to the limitation of Euler-Bernoulli beam theory.

5.2.2 Case 2 (Keeping Ω fixed and vary ω_{str})

Fig. 5 shows that as ω_{str} increases, the spectrum relation becomes more dispersive and also the difference between c and c_g rise. So the input signal cannot maintain its shape as it travels along the beam. As discussed earlier, when ω_{str} decreases, the wavenumber increases and hence the wave propagation speed decreases.

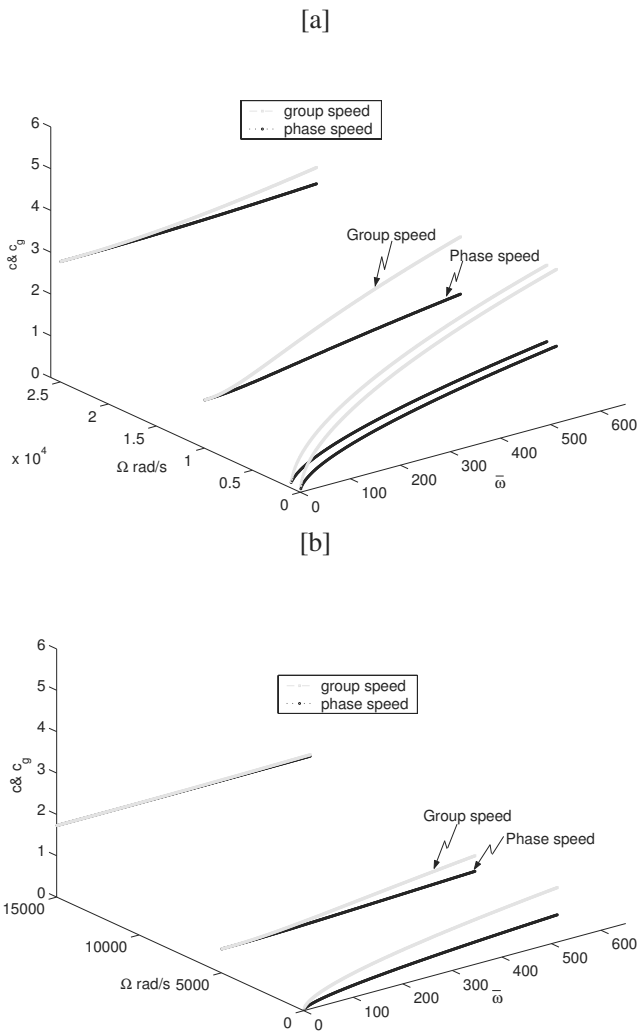

Figure 4 : Variation of $\overline{c}$ and $\overline{c}_g$wrt. $\overline{\omega}$ and Ω keeping ω_{str} constant (a)Euler beam1, L $0.6m$, mass $1.128kg$, ω_{str} $5.198rad/s$, ω_1 (first sampling frequency) $6.136e3rad/s$ (b) Euler beam2, L $4.94m$, mass $31.924kg$, ω_{str} $5.198rad/s$, ω_1 $6.136e3rad/s$

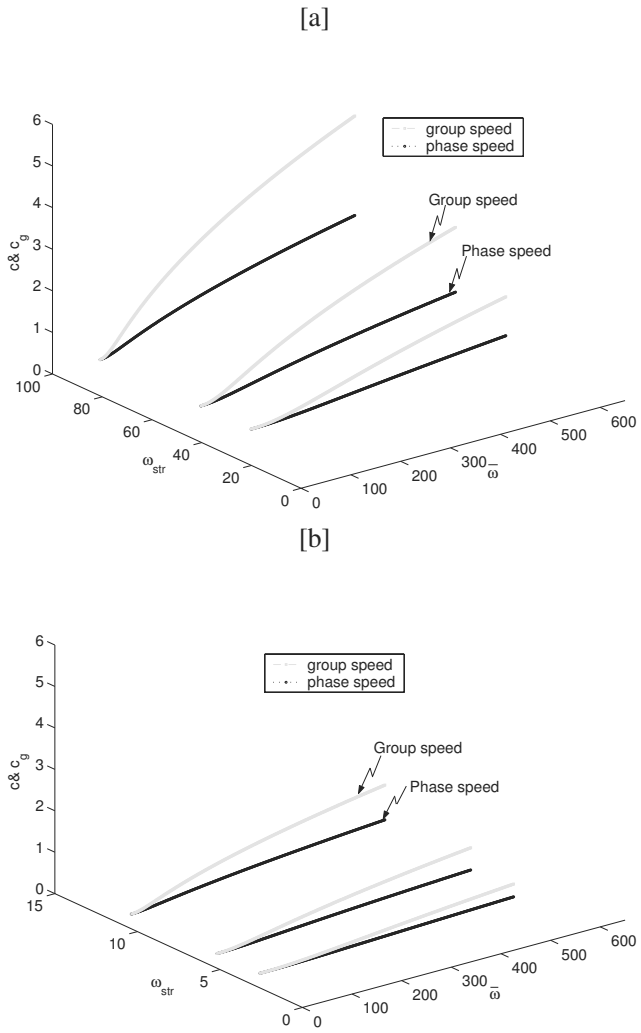

Figure 5 : Variation of $\overline{c}$ and $\overline{c}_g$wrt. $\overline{\omega}$ and ω_{str} keeping Ω constant (a)Euler beam1, L $0.6m$, mass $1.128kg$, Ω $7500rad/s$, ω_1 (first sampling frequency) $6.136e3rad/s$ (b)Euler beam2, L $4.94m$, mass $31.924kg$, Ω $3000rad/s$, ω_1 $6.136e3rad/s$

The variation of non-dimensional group speed and phase speed with respect to rotation, for a given sampling frequency is illustrated using the Euler beam2 properties. Fig. 6a shows that when the sampling frequency is $3e4rad/s$, the c and c_g matches except at low rotation speeds. This is in good agreement with the result shown in Fig. 4. Fig. 6b shows that for the higher frequency, $3e6rad/s$, difference between c and c_g exists up to certain Ω, and the difference tends to zero at very high rotation speeds. As mentioned earlier, it is very clear from these plots that for non-rotating beams, the group speed is twice that of phase.

5.3 Impact response

High frequency content, short duration pulse as shown in Fig. 7a is given at the beam tip. Fig. 7b shows the FFT of the pulse or the input amplitude spectrum $\hat{F}_2$. The Eq. 46 is evaluated for each sampling frequency up to the Nyquist frequency to obtain $\overline{W}_3$. The inverse transform of the product $(j\overline{\omega}\overline{W}_3)$ gives the non-dimensional transverse velocity of the beam at $X = 1$. The non-dimensional transverse velocity $\overline{v}$, at the impact location

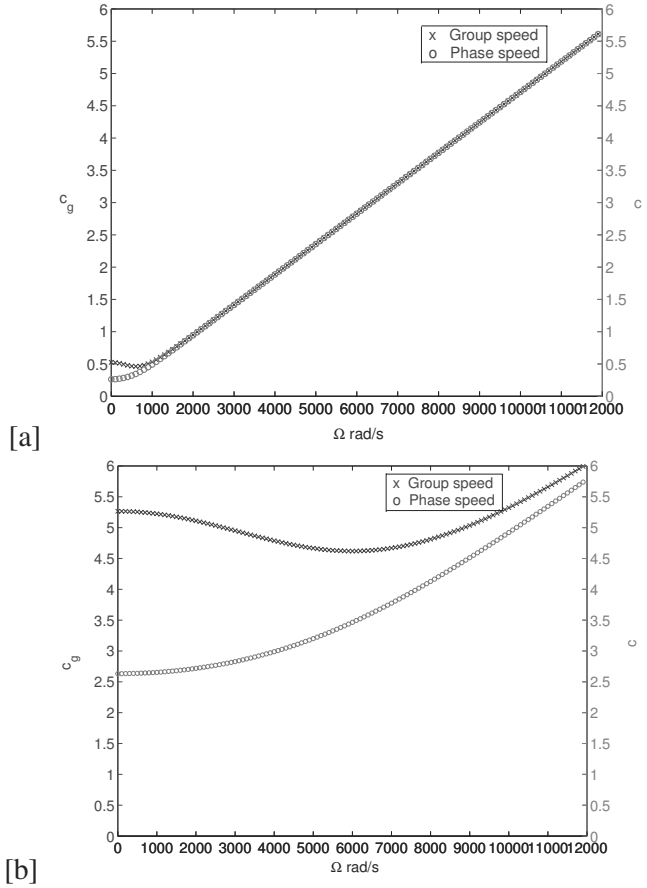

Figure 6 : Variation of $\overline{c}$ and $\overline{c}_g$wrt. Ω for a given ω (a)Euler beam2 L $4.94m$, mass $31.924kg$, ω_{str} $5.198rad/s$, ω $3e4rad/s$ (b) Euler beam2 L $4.94m$, mass $31.924kg$, ω_{str} $5.198rad/s$, ω $3e6rad/s$

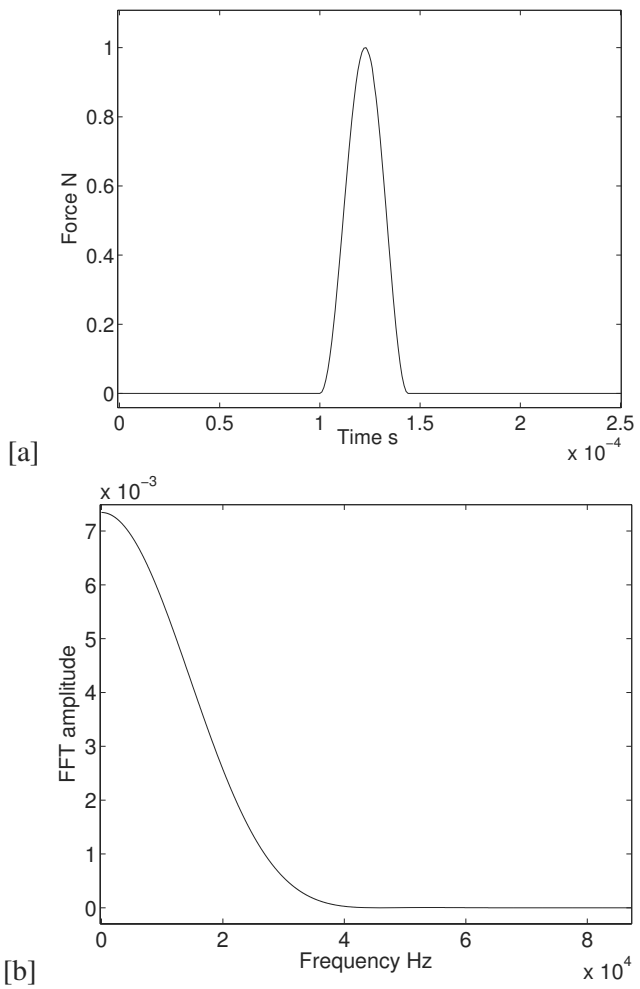

Figure 7 : (a)Input force pulse (b) FFT of the input force pulse

is plotted and the wave characteristics studied by changing Ω and ω_{str} independently.

5.3.1 Case 1 (Keeping ω_{str} fixed and vary Ω)

Fig. 8 show that the velocity amplitude is directly dependent on Ω. When rotation speed increases, the wavenumber decreases and the spectrum relation becomes non-dispersive. One can observe a steep increase in response amplitude with increase in rotation speed and also the incident response peek vanishes. Due to the linear spectrum relation at higher Ω, the reflected signal could retain the same shape as the input signal and the same can be observed from the plot. Furthermore, the time taken for reflection decreases due to the reduction in wavenumber and the consequent increase in the wave propagation speed.

5.3.2 Case 2 (Keeping Ω fixed and vary ω_{str})

From Fig. 9 it is apparent that the velocity amplitude changes inversely with ω_{str}. Reduction in transverse displacement amplitude, due to increased flexural stiffness of the beam, decreases the transverse velocity. Also, from the wavenumber plot it is understood that spectrum relation is quadratic and the wavenumber reduces at higher values of ω_{str}. As a result, the spectrum relation becomes dispersive and the wave propagation velocity increases at higher ω_{str}. This can be verified by observing the propagation time taken by the reflected signal.

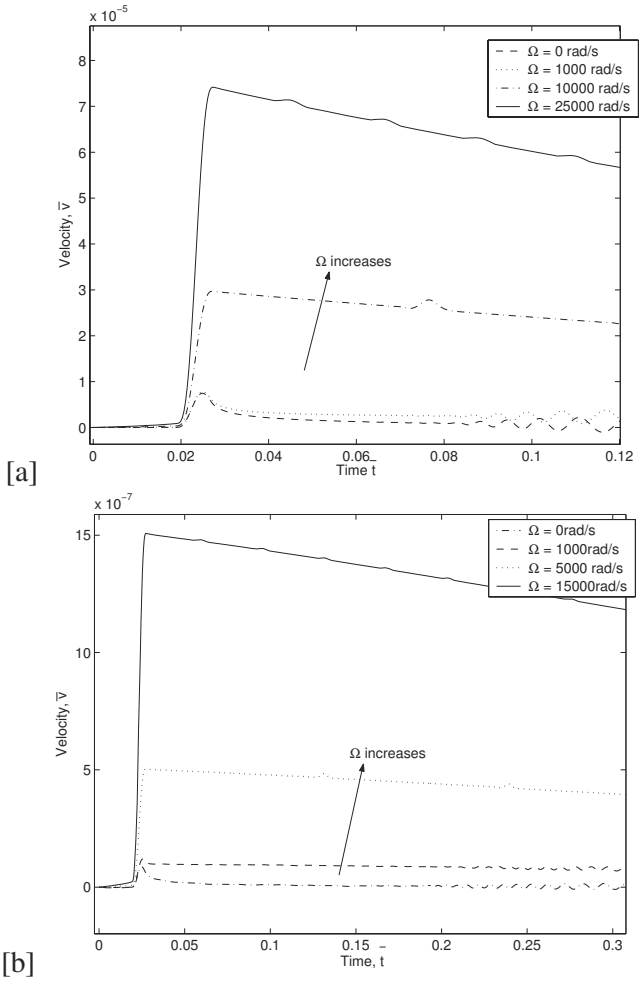

Figure 8 : Non-dimensional impulse response for different Ω keeping ω_{str} constant. (a)Euler beam1, L $0.6m$, mass $1.128kg$, ω_{str} $40.5rad/s$, ω_1 (first sampling frequency) $6.136e3rad/s$ (b) Euler beam2, L $4.94m$, mass $31.924kg$, ω_{str} $5.198rad/s$, ω_1 $6.136e3rad/s$

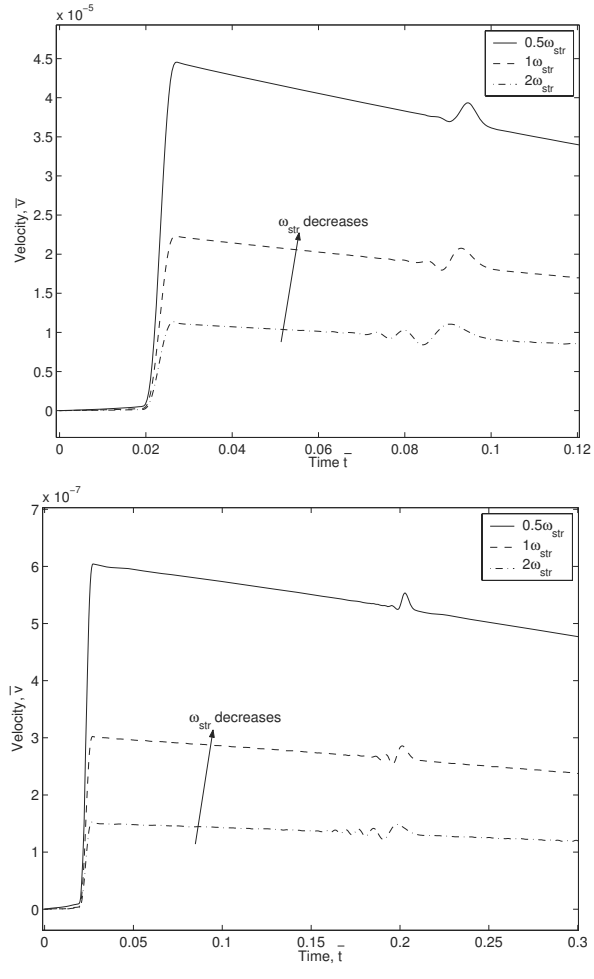

Figure 9 : Non-dimensional impulse response for different ω_{str} keeping Ω constant. (a)Euler beam1, L $0.6m$, mass $1.128kg$, ω_{str} $40.5rad/s$, ω_1 (first sampling frequency) $6.136e3rad/s$ (b) Euler beam2, L $4.94m$, mass $31.924kg$, ω_{str} $5.198rad/s$, ω_1 $6.136e3rad/s$

6 Conclusion

An effort is made to study the wave propagation characteristics of a uniform beam with axial force proportional to rotation speed, using the spectral finite element method (SFEM). The governing PDE is derived using the Euler-Bernoulli beam theory and Hamilton's principle. The system transfer function in the frequency domain is obtained using the spectral approach along with the boundary conditions. The wavenumber is calculated from the coefficients of the governing differential equation in the spectral form and the sampling frequency. The dependence of wavenumber on the centrifugal force term and the beam flexural stiffness is investigated. The dispersive spectrum relation of non-rotating beam transforms to non-dispersive at high rotation speeds. The wave propagation speed increases with the rotation speed and beam flexural stiffness.

The beam is subjected to an impact load and the response is analyzed for different rotation speeds and beam stiffness using two numerical examples, in a qualitative way. The study reveals the effect of rotation speed on the response and wave propagation behavior of the beam. The transverse velocity amplitude rises with the rotating speed and declines with the beam flexural stiffness. The time of reflection of the input pulse decreases with in-

creasing rotation speed and flexural stiffness. The input pulse retains its original shape at high rotation speeds, even after multiple reflections. Again, at high rotation speeds, the reflected signal vanishes in the transverse velocity response of the beam.

The solution from the present model can also be used as the approximate solution to the problem where the variable coefficients due to centrifugal stiffening, mass variation or flexural rigidity are present. Assuming the solution obtained from this paper as the Ritz functions for the variable coefficient ODE, the dynamic stiffness matrix in the frequency domain can be obtained using the principle of stationary potential energy (Gopalakrishnan and Doyle (1994)). The accuracy of this approach improves with the number of degrees of freedom or with the number of elements used. Thus, it is advantageous that the variable coefficient ODE need not be solved using the Frobenius method, which requires about 80 to 350 terms of the Frobenius series, for higher accuracy (Banerjee (2000); Wang and Wereley (2004)). This shows the relevance of the present study in the analysis of rotating beam problems using the spectral method.

References

Andreaus, U.; Batra, R. C.; Porfiri, M. (2005): Vibrations of Cracked Euler-Bernoulli Beams using Meshless Local Petrov-Galerkin (MLPG) Method. *CMES: Computer Modeling in Engineering and Sciences*, vol. 9, no. 2, pp. 111–132.

Banerjee, J. R. (2000): Free vibration of centrifugally stiffened uniform and tapered beams using the dynamic stiffness method. *Journal of Sound and Vibration*, vol. 233, no. 5, pp. 857–875.

Chakraborty, A.; Gopalakrishnan, S. (2003): A spectrally formulated finite element for wave propagation analysis in functionally graded beams. *International Journal of Solids and Structures*, vol. 40, pp. 2421–2448.

Chakraborty, A.; Gopalakrishnan, S. (2005): A spectral finite element for axial-flexural-shear coupled wave propagation analysis in lengthwise graded beam. *Comput. Mech.*, vol. 36, pp. 1–12.

Doyle, J.; Farris, T. (1990): A spectrally formulated element for flexural wave propagation in beams. *International Journal of Analytical and Experimental Modal Analysis*, vol. 3, pp. 1–5.

Doyle, J. F. (1988): A spectrally formulated finite element for longitudinal wave propagation. *International Journal of Analytical and Experimental Modal Analysis*, vol. 5, pp. 99–107.

Doyle, J. F. (1989): Wave Propagation in Structures: an FFT based spectral analysis methodology. *Springer-Verlag*.

Fedelinski, P.; Gorski, R. (2006): Analysis and optimization of Dynamically Loaded Reinforced Plates by the Coupled Boundary and Finite Element Method. *CMES: Computer Modeling in Engineering and Sciences*, vol. 15, no. 1, pp. 31–40.

Forth, S. C.; Staroselsky, A. (2005): A Hybrid FEM/BEM Approach for Designing an Aircraft Engine Structural Health Monitoring . *CMES: Computer Modeling in Engineering and Sciences*, vol. 9, no. 3, pp. 287–298.

Gopalakrishnan, S.; Doyle, J. F. (1994): Wave propagation in connected waveguides of varying cross-section. *Journal of Sound and Vibration*, vol. 175, no. 3, pp. 347–363.

Gopalakrishnan, S.; Martin, M.; Doyle, J. F. (1992): A matrix methodology for spectral analysis of wave propagation in multiple connected Timoshenko beams. *Journal of Sound and Vibration*, vol. 158, no. 1, pp. 11–24.

Han, X.; Ding, H.; Liu, G. R. (2005): Elastic waves in a hybrid multilayered piezoelectric plate. *CMES: Computer Modeling in Engineering and Sciences*, vol. 9, no. 1, pp. 49–56.

Hoa, S. V. (1979): Vibration of a rotating beam with tip mass. *Journal of Sound and Vibration*, vol. 67, pp. 369–381.

Huston, R. L.; Liu, C. Q. (2005): Advances in Computational Methods for Multibody System Dynamics. *CMES: Computer Modeling in Engineering and Sciences*, vol. 10, no. 2, pp. 143–152.

Leu, S. Y.; Chen, J. T. (2006): Sequential Limit Analysis of Rotating Hollow Cylinders of Nonlinear Isotropic Hardening . *CMES: Computer Modeling in Engineering and Sciences*, vol. 14, no. 2, pp. 129–140.

Mahapatra, D. R.; Gopalakrishnan, S. (2000): Spectral-element-based solutions for wave propagation analysis of multiply connected unsymmetric laminated composite beams. *Journal of Sound and Vibration*, vol. 237, no. 5, pp. 819–836.

Mahapatra, D. R.; Gopalakrishnan, S. (2003): A spectral finite element model for analysis of axial-flexural-shear coupled wave propagation in laminated composite beams. *Composite Structures*, vol. 59, pp. 67–88.

Martin, M.; Gopalakrishanan, S.; Doyle, J. (1994): Wave propagation in multiply connected deep wave guides. *Journal of Sound and Vibration*, vol. 174, no. 4, pp. 521–538.

Mitra, M.; Gopalakrishnan, S. (2006): Wavelet Based 2-D Spectral Finite Element Formulation for Wave Propagation Analysis in Isotropic Plates . *CMES: Computer Modeling in Engineering and Sciences*, vol. 15, no. 1, pp. 49–68.

Nagaraj, V. T.; Kumar, P. S. (1975): Rotor blade vibrations by the Gelerkin finite element method. *Journal of Sound and Vibration*, vol. 43, no. 3, pp. 575–577.

Naguleswaran, N. (1994): Lateral vibration of a centrifugally tensioned uniform Euler-Bernoulli beam. *Journal of Sound and Vibration*, vol. 176, no. 5, pp. 613–624.

Narayanan, G. V.; Beskos, D. E. (1982): Numerical operational methods for time-dependant linear problems. *International Journal for Numerical Methods in Engineering*, vol. 18, pp. 1829–1854.

Pawar, P. M.; Ganguli, R. (2003): Genetic fuzzy system for damage detection in beams and helicopter rotor blades. *Comput. Methods Appl. Mech. Engrg.*, vol. 192, pp. 2031–2057.

Pluymers, B.; Desmet, W.; Vandepitte, D.; Sas, P. (2005): On the use of a wave based prediction technique for steady-state structural-acoustic radiation analysis. *CMES: Computer Modeling in Engineering and Sciences*, vol. 7, no. 2, pp. 173–184.

Putter, S.; Manor, H. (1978): Natural frequencies of radial rotating beams. *Journal of Sound and Vibration*, vol. 56, pp. 175–185.

Wang, G.; Wereley, N. M. (2004): Free vibration analysis of rotating blades with uniform tapers. *AIAA Journal*, vol. 42, no. 12, pp. 2429–2437.

Wright, A. D.; Smith, C. E.; Thresher, R. W.; Wang, J. L. C. (1982): Vibration modes of centrifugally stiffened beams. *Journal of Applied Mechanics*, vol. 49, no. 2, pp. 197–202.

Wu, C. Y.; Liu, X. Y.; Scarpas, A.; Ge, X. R. (2006): Spectral Element Approach for Forward Models of 3D Layered Pavement. *CMES: Computer Modeling in Engineering and Sciences*, vol. 12, no. 2, pp. 149–158.